Research Article Vol. 2, No. 2 / 15 February 2019 / OSA Continuum 236

Optical parametric amplification of a Laguerre–Gaussian mode

XINYUAN FANG,[1,3] HAOCHENG YANG,[1,3] YONG ZHANG,[1,*] AND MIN XIAO[1,2]

[1] National Laboratory of Solid State Microstructures, College of Engineering and Applied Sciences, and School of Physics, Nanjing University, Nanjing 210093, China
[2] Department of Physics, University of Arkansas, Fayetteville, Arkansas 72701, USA
[3] These authors contributed equally.
[*] zhangyong@nju.edu.cn

Abstract: We theoretically study the optical parametric amplification (OPA) process seeded by a Laguerre–Gaussian (LG) mode. Based on the nonlinear coupled-wave equations, we analyze the overlap integral among interacting LG beams, which presents the selection laws for the azimuthal and radial indices of a pure LG mode in the OPA process. In the numerical simulations, we demonstrate the amplification of an LG_{01} mode as an example with high purity and high gain. Our results provide a potential way to efficiently amplify an LG mode for optical communications.

© 2019 Optical Society of America under the terms of the OSA Open Access Publishing Agreement

1. Introduction

In 1992, Allen *et al.* pointed out that light beams featuring helical wavefronts [1], such as Laguerre–Gaussian (LG) beams, carry orbital angular momentum (OAM). Since then, LG beams have attracted significant attention from researchers worldwide, owing to their widespread applications in optical tweezers [2,3], optical trapping [4], imaging [5], astronomy [6], rotation measurement [7], and quantum information processing [8–13]. In particular, owing to the unbounded set of OAM states, OAM multiplexing has largely been explored for optical communications [14,15], indicating that the LG beam is a promising candidate for dramatically boosting the capacities of communication systems. However, the propagation loss in long distance communication will degrade the performance. The second-order nonlinear process, *i.e.*, optical parametric amplification (OPA), provide a potential method for amplifying the LG modes.

Many interesting experiments have been performed to demonstrate the conversion of the azimuthal index (l), *i.e.*, the OAM number, of an LG mode during nonlinear optical processes, such as second harmonic generation (SHG), third harmonic generation (THG), four-wave mixing (FWM), spontaneous parametric down conversion (SPDC), and optical parametric oscillator (OPO) [16–24]. The OAM conservation law has been confirmed in most nonlinear optical processes. However, the conversion of the radial index (m) of an LG mode is rarely investigated [25,26]. This is particularly meaningful in the OPA process, because it is directly associated with the purity of the amplified LG modes. A pure LG beam (normally with $m = 0$) promises to be applied in a variety of fields, such as the improvement of signal-to noise ratio in optical communication, the design of OAM-multiplexed holograms and so forth. It should be noted that the non-zero radial index of LG mode is usually considered as noise in most of above practical applications. Our simulations show that the spatial modes of the output signal strongly depend on the pump modes. One should choose the appropriate pump beam to amplify an LG mode without introducing unexpected radial components.

In this paper, we investigate the collinear optical parametric amplification process seeded by a pure LG mode. Based on the calculation of the spatial overlap integration between the modes participating in the three-wave mixing process, we achieve the mode selection rules for both the azimuthal and radial indices. As an example, we take LG_{01} ($m = 0$, $l = 1$) mode as the input

#342747 https://doi.org/10.1364/OSAC.2.000236
Journal © 2019 Received 20 Aug 2018; revised 6 Dec 2018; accepted 6 Dec 2018; published 15 Jan 2019

OSA CONTINUUM

signal and study its gain and purity pumped by different LG modes. The theoretical analysis can be readily extended to the amplification of other LG modes. Moreover, we analyze the influences of the crystal length on the output signal in such OPA process. These results embody interesting regularity, which may be helpful to understand the essence of the m index in an LG-mode.

2. Mathematical model

OPA is a three-wave mixing nonlinear optical process in which a strong pump light at frequency ω_p and a weak seed light at frequency ω_s interact in a nonlinear optical medium to produce an amplified ω_s and an idler light at $\omega_i = \omega_p - \omega_s$. In a cylindrical coordinate system where light beams propagate along the z axis, the coupled wave equations for an OPA process can be written as [27]

$$\begin{aligned}
\nabla^2 E_s(r,z) + k_s^2 E_s(r,z) &= -\frac{2\chi^{(2)}\omega_s^2}{c^2} E_p E_i^* \\
\nabla^2 E_i(r,z) + k_i^2 E_i(r,z) &= -\frac{2\chi^{(2)}\omega_i^2}{c^2} E_p E_s^* \\
\nabla^2 E_p(r,z) + k_p^2 E_p(r,z) &= -\frac{2\chi^{(2)}\omega_p^2}{c^2} E_s E_i
\end{aligned} \tag{1}$$

Here, p, s, and i denote the pump, signal (seed), and idler, respectively, E is the electrical field, $\chi^{(2)}$ is the second-order nonlinear coefficient, and k is the wave number. Considering the OPA process with LG modes, we use the cylindrical coordinates in the theoretical model. The field E_j ($j = p$, s, or i) can be expanded as [28]

$$E_j = \sum B_j(z) u_{ml}^j(r,z) e^{ik_j z} \tag{2}$$

where $u_{ml}^j(r, z)$ represents an LG mode with the radial index m and azimuthal index l, and $B_j(z)$ is the field envelope of an LG mode. In the cylindrical coordinates, the expression for $u_{ml}^j(r, z)$ is given by [28]

$$u_{ml}^j = \sqrt{\frac{2}{\pi}} \times \frac{N_{ml}}{w_j} \left(\frac{\sqrt{2}r}{w_j}\right)^{|l|} L_m^{|l|}\left(\frac{2r^2}{w_j^2}\right) \exp\left[i\left(\frac{k_j r^2}{2\bar{z}} - (2m + |l| + 1)\arctan\left(\frac{z}{z_R}\right) + l\theta\right)\right] \tag{3}$$

Here, $\sqrt{\frac{2}{\pi}} \times \frac{N_{ml}}{w_j}$ is the normalized coefficient with $N_{ml} = \sqrt{\frac{m!}{(m+|l|)!}}$ and $w_j = w_{j0}\sqrt{1 + \left(\frac{z}{z_R}\right)^2}$, w_{j0} is the beam waist, z_R is the Rayleigh range, and $\bar{z} = z - iz_R$.

By substituting Eq. (2) into Eq. (1), performing the transformation $B_{ml}(z) = \sqrt{\frac{\omega}{n}} A_{ml}(z)$ [28], and considering the orthogonality of the LG modes, the following coupled wave equations involving transverse modes are acquired (we consider the phase-matched case, *i.e.*, $\Delta k = k_p - k_s - k_i = 0$),

$$\begin{aligned}
\frac{\partial A_{m_s l_s}}{\partial z} &= \frac{i\chi^{(2)}}{c}\sqrt{\frac{\omega_p\omega_s\omega_i}{n_p n_s n_i}} \left(\sum \Lambda_{m_p m_s m_i}^{l_p l_s l_i} A_{m_p l_p} A_{m_i l_i}^*\right) \\
\frac{\partial A_{m_i l_i}}{\partial z} &= \frac{i\chi^{(2)}}{c}\sqrt{\frac{\omega_p\omega_s\omega_i}{n_p n_s n_i}} \left(\sum \Lambda_{m_p m_s m_i}^{l_p l_s l_i} A_{m_p l_p} A_{m_s l_s}^*\right) \\
\frac{\partial A_{m_p l_p}}{\partial z} &= \frac{i\chi^{(2)}}{c}\sqrt{\frac{\omega_p\omega_s\omega_i}{n_p n_s n_i}} \left(\sum \left(\Lambda_{m_p m_s m_i}^{l_p l_s l_i}\right)^* A_{m_s l_s} A_{m_i l_i}\right)
\end{aligned} \tag{4}$$

Here, the overlap integral is defined by

$$\Lambda_{m_p m_s m_i}^{l_p l_s l_i} = \iint u_{m_p l_p} u_{m_s l_s}^* u_{m_i l_i}^* r dr d\theta = 2\pi\delta_{l_p, l_s + l_i} \int_0^\infty u_{m_p l_p} u_{m_s l_s}^* u_{m_i l_i}^* r dr \tag{5}$$

The overlap integral is a crucial factor for a parametric process involving LG modes because it decides the conversion efficiency. Note that $\delta_{lp,ls+li}$ in Eq. (5) actually implies the selection rule

OSA CONTINUUM

for the azimuthal index l of LG modes, *i.e.*, l_p=l_s+l_i [29]. However, the selection rule for the radial index m of the LG mode is not clear. Next, we develop a complete set of selection rules for the m index from Eq. (5).

We consider a pure LG seed mode with $m_s = 0$. With the help of the generating function and polynomial identity theorem [29], the analytical expression of the integral in Eq. (5) can be written as

$$\begin{aligned}\int_0^\infty u_{m_p l_p} u^*_{0,l_s} u^*_{m_i l_i} r dr &= Const \int \left(\sqrt{2}r\right)^{|l_p|+|l_s|+|l_i|} L_{m_p}^{|l_p|}\left(\tfrac{2r^2}{w_p(z)^2}\right) L_{m_i}^{|l_i|}\left(\tfrac{2r^2}{w_i(z)^2}\right) \exp\left(-\tfrac{2r^2}{w_p(z)^2}\right) r dr \\ &= Const 2 \times \Gamma(\lambda+1)\left[\sum_k \binom{-\lambda-1}{k}\left(\sum_j \binom{k}{j}\left((\eta-1)^k \binom{\lambda-\mu'}{n'-k}\left(\tfrac{\eta}{\eta-1}\right)^j \binom{\lambda-\mu}{n-j}\right)\right)\right](-1)^{n'+n}\end{aligned} \tag{6}$$

where $\lambda = (|l_p|+|l_s|+|l_i|)/2$, $n = m_p$, n '$=m_i$, $\mu = |l_p|$, $\mu' = |l_i|$, $\eta = (w_p(z)/w_i(z))^2$. Here, we assume the Rayleigh ranges for pump, signal and idler beams are the same [29].

The function $\binom{a}{b}$ is defined by

$$\binom{a}{b} = \begin{cases} \frac{a!}{b!(a-b)!}, a > b \\ 0, \ a < b \end{cases} \tag{7}$$

Therefore, the inequalities $\lambda-\mu' > n'-k$ and $\lambda-\mu > n-j$ must hold. When inputting a LG mode with $m_s = 0$, the selection rules for the index m can be summarized as

1) If $l_s \cdot l_i < 0$, $m_p = 0, 1, \ldots,$ min $|l_s|, |l_i|$; otherwise, $m_p = 0$.

2) If $l_p \cdot l_s > 0$, $m_i = 0, 1, \ldots,$ min $|l_p|, |l_s|$; otherwise, $m_i = 0$.

3) If $l_p \cdot l_i > 0$, $m_s = 0, 1, \ldots,$ min $|l_p|, |l_i|$; otherwise, $m_s = 0$.

3. Numerical simulation results

As an example, we numerically simulate an OPA process in which a seed LG_{01} mode with $m_s = 0$ and $l_s = 1$ is amplified. The wavelengths for the pump and seed are 532 nm and 1064 nm, respectively. We consider a case of noncritical phase matching in a 12 mm-long lithium triborate (LBO) crystal. The refractive indexes for the pump and signal lights are $n_p = n_s = 1.6$, and the nonlinear coefficient is $d = 0.83$ pm/V[30].

In light of the above selection rules, given a pump with certain m_p and l_p, one can determine all the possible m_s, l_s, m_i, and l_i in the output signal. First, we decide the input m_p for the amplification of LG_{01} mode. From the selection rule 1) for m index, if $l_p \geq 1$, m_p must be 0, and if $l_p < 1$, m_p can be 0 or 1. However, due to the existence of the term (-1) $^{n'+n}$ in Eq. (6), the calculated overlap integrals from Eq. (5) for $m_p = 0$ and $m_p = 1$ have different signs. Obviously, a destructive interference will occur between the signals generated by these two pump modes, leading to a decrease in the signal gain. Therefore, in the following theoretical simulations, we only employ a pump mode with m_p=0 to amplify the seed light. For example, consider a pump with $m_p = 0$ and $l_p = 3$. According to the conservation of l index, it must hold that $l_i = 2$ because $l_s = 1$. From the selection rules 2) and 3) for m index, one can obtain that m_i can be 0 or 1, and m_s can be 0, 1, or 2. There are six mode components in the generated signal and idler lights. Their ratios can be calculated from Eq. (5).

Next, we numerically simulate the cases in which m_p=0 and l_p takes a value from -2 to 3. Figure 1 depicts the variation of the output signal intensity (I_s) with the crystal length. It should be noted that a certain incident pump mode may generate multiple signal modes with the same l_s but different m_s. The signal intensity in Fig. 1 includes all the generated signal modes. It is

OSA CONTINUUM

observed that when the incidental l_p is negative the total signal gain is quite low. When using a positive l_p, the total signal gain is relatively high.

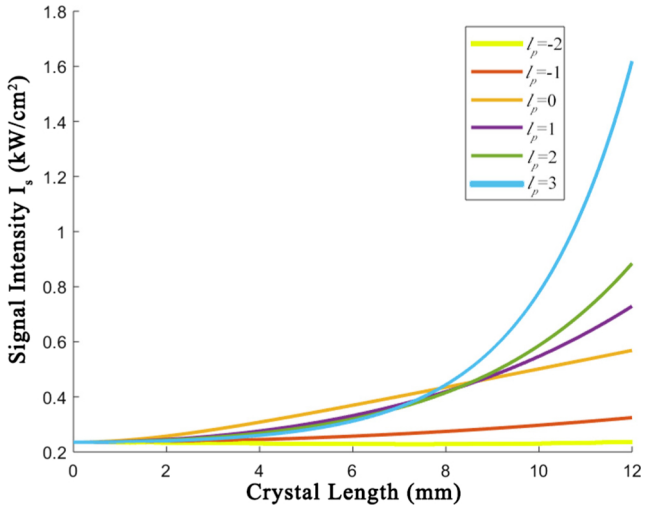

Fig. 1. Signal intensity I_s versus crystal length for various pump modes with $l_p = -2$ to 3.

Figure 2 shows the simulated intensity patterns of the amplified signals when different pump modes are involved. We also analyze the mode components of the signals (Fig. 3). Since the goal is to amplify an LG_{01} mode, the mode purity is defined by the ratio between I_s ($m_s = 0$) and the total I_s. The patterns for $l_p = 2$ and 3 in Fig. 2 are different from the others because of the low mode purity of the amplified signal. By analyzing the simulation results in Figs. 1 and 3, we conclude that when $l_p \leq 1$ the amplified signal mode has high purity, while the total signal gain is high with a pump mode of $l_p \geq 0$. The pump light with a large l_p (for example, $l_p = 3$) results in a low signal purity but a high gain, indicating that the high-order LG components have a significant consumption of the pump energy. This should be carefully avoided when one cares the purity of the amplified signal.

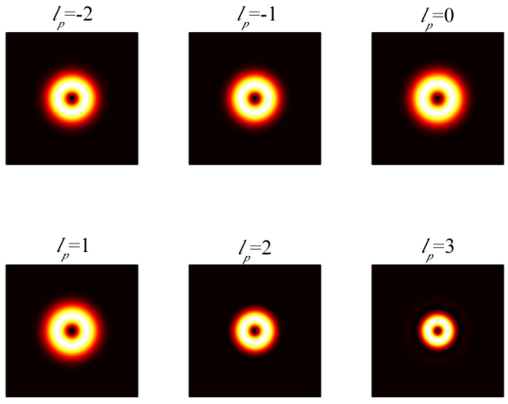

Fig. 2. Simulated intensity patterns of the amplified signals corresponding to different pump modes.

By distinguishing the mode components in signal lights, we are able to numerically evaluate the intensity dependence of the pure output LG_{01} signal on the crystal length (Fig. 4). Because

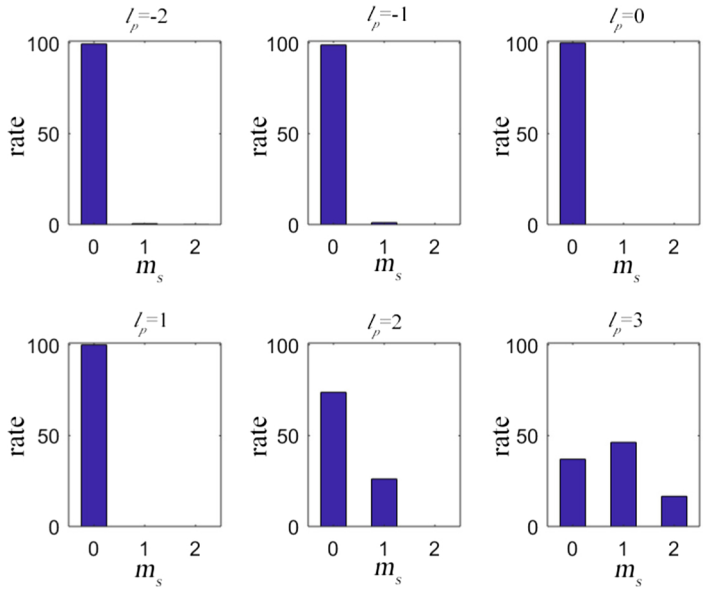

Fig. 3. Rates of different signal modes when different pumps are employed.

the total signal gain with $l_p < 0$ is very low, we only study the cases with $l_p \geq 0$. As shown in Fig. 4, the pump mode with $m_p = 0$ and $l_p = 1$ is an optimal choice for efficient amplification of a pure LG mode. In addition, when using a 50 mm-long nonlinear crystal, the conversion efficiency for pure LG_{01} signal can be significant enhanced with a pump light of $m_p = 0$ and $l_p = 1$ (yellow line in Fig. 5(a)). In the other cases, the intensity of LG_{01} signal component present oscillations (Fig. 5(a)).

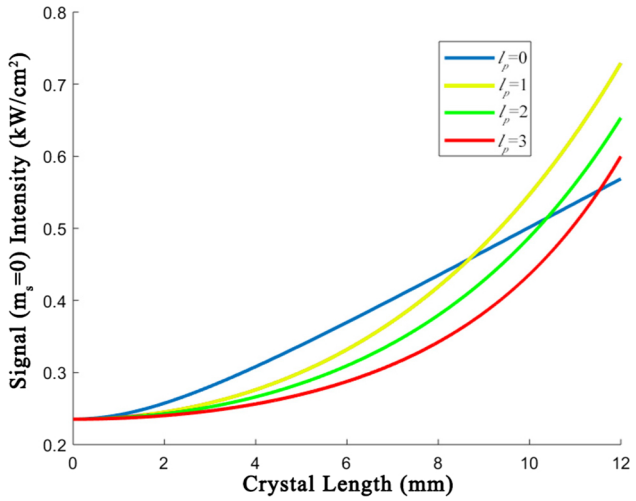

Fig. 4. The intensity of pure LG_{01} signal ($m_s = 0$) versus crystal length.

We perform further simulations to analyze the origination of the oscillations in Fig. 5(a). Figures 5(b) and 5(c) show the evolution of all the other possible high-order signal mode, *i.e.*, LG_{11} ($m_s = 1$) and LG_{21} ($m_s = 2$) modes, along the crystal length. Clearly, under a given pump

OSA CONTINUUM

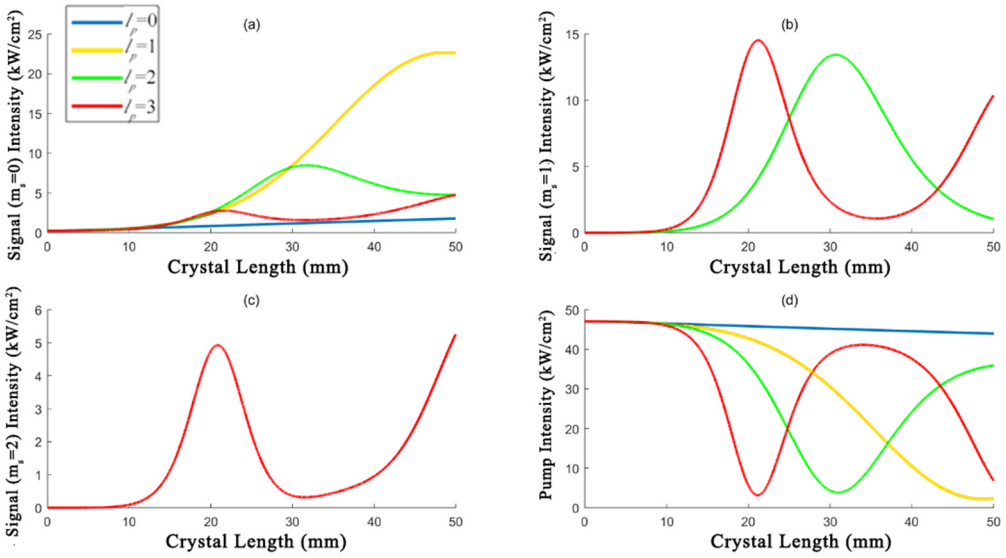

Fig. 5. (a) Pure signal ($m_s = 0$) intensity versus crystal length. (b) Signal ($m_s = 1$) intensity versus crystal length. (c) Signal ($m_s = 2$) intensity versus crystal length. (d) Total pump intensity versus crystal length.

mode, all the mode components in the amplified signal reach their maximal intensity at the same crystal length. For example, using a pump mode of $m_p = 0$ and $l_p = 3$ (see the red lines in Figs. 5(a)–(c)), the signal intensities with $m_s = 0$, 1, and 2 simultaneously reach their maximum at the crystal length of 21.1 mm. This rules out the possibility of mode competitions during nonlinear conversion. Figure 5(d) shows the evolution of the pump intensity along the crystal length. Under a certain pump condition, for example, $m_p = 0$ and $l_p = 2$, the pump intensity reaches its minimum at the crystal length of 31.1 mm, where the signal intensity is in its maximal value (the green lines in Figs. 5(a), (b), and (d)). Therefore, the oscillation in the signal intensity can be attributed to the energy backflow in the OPA process. After carefully examining the yellow lines in Figs. 5(a) and 5(d), one can find that, the energy reflux also happens under a pump light of $m_p = 0$ and $l_p = 1$, except that the gain is much higher and the oscillations presents at a longer crystal length (~48 mm) compared to the other pump case.

4. Conclusion

We have theoretically studied the LG mode amplification through an OPA process based on nonlinear coupled wave equations. By analyzing the overlap integral in the three-wave mixing, we demonstrate the conservation law of the azimuthal index and the spatial mode selection law of the radial index. In numerical simulations, we show that the pump mode with $m_p = 0$ and $l_p = 1$ is an optimal choice to amplify an LG_{01} mode with a high purity and a high gain. Our result promises to be helpful in various practical and theoretical situations, including signal enhancement in LG-mode based optical communication, the design of OAM based holograms and the physical understanding of the m index of an LG-mode.

Funding

National Natural Science Foundation of China (NSFC) (11621091, 11874213, 91636106); National Key R&D Program of China (2016YFA0302500, 2017YFA0303703); Fundamental

OSA CONTINUUM

Research Funds for Central Universities (021314380105); Dengfeng Project B of Nanjing University.

References

1. L. Allen, M. W. Beijersbergen, R. J. C. Spreeuw, and J. P. Woerdman, "Orbital angular momentum of light and the transformation of Laguerre-Gaussian laser modes," Phys. Rev. A **45**(11), 8185–8189 (1992).
2. D. G. Grier, "A revolution in optical manipulation," Nature **424**(6950), 810–816 (2003).
3. S. Tao, X. C. Yuan, J. Lin, X. Peng, and H. Niu, "Fractional optical vortex beam induced rotation of particles," Opt. Express **13**(20), 7726–7731 (2005).
4. M. P. MacDonald, L. Paterson, K. Volke-Sepulveda, J. Arlt, W. Sibbett, and K. Dholakia, "Creation and manipulation of three-dimensional optically trapped structures," Science **296**(5570), 1101–1103 (2002).
5. A. Jesacher, S. Furhapter, C. Maurer, S. Bernet, and M. Ritsch-Marte, "Holographic optical tweezers for object manipulations at an air-liquid surface," Opt. Express **14**(13), 6342–6352 (2006).
6. D. Hetharia, M. P. van Exter, and W. Löffler, "The Role of Spatial Coherence and Orbital Angular Momentum of Light in Astronomy," Phys. Rev. A **90**(6), 063801 (2014).
7. S. Xiao, L. D. Zhang, D. Wei, F. Liu, Y. Zhang, and M. Xiao, "Orbital angular momentum-enhanced measurement of rotation vibration using a Sagnac interferometer," Opt. Express **26**(2), 1997 (2018).
8. A. Mair, A. Vaziri, G. Weihs, and A. Zeilinger, "Entanglement of the orbital angular momentum states of photons," Nature **412**(6844), 313–316 (2001).
9. A. C. Dada, J. Leach, G. S. Buller, M. J. Padgett, and E. Andersson, "Experimental high-dimensional two-photon entanglement and violations of generalized Bell inequalities," Nat. Phys. **7**(9), 677–680 (2011).
10. J. T. Barreiro, T. C. Wei, and P. G. B. Kwiat, "Beating the channel capacity limit for linear photonic superdense coding," Nat. Phys. **4**(4), 282–286 (2008).
11. D. S. Ding, Z. Y. Zhou, B. S. Shi, and G. C. Guo, "Single-photon-level quantum image memory based on cold atomic ensembles," Nat. Commun. **4**(1), 2527 (2013).
12. G. Molina-Terriza, J. P. Torres, and L. Torner, "Twisted photons," Nat. Phys. **3**(5), 305–310 (2007).
13. J. Guo, C. Cai, L. Ma, K. Liu, H. Sun, and J. Gao, "Higher order mode entanglement in a type II optical parametric oscillator," Opt. Express **25**(5), 4985 (2017).
14. A. Trichili, C. Rosales-Guzman, A. Dudley, B. Ndagano, A. B. Salem, M. Zghal, and A. Forbes, "Optical communication beyond orbital angular momentum," Sci. Rep. **6**(1), 27674 (2016).
15. G. Xie, Y. Ren, Y. Yan, H. Huang, N. Ahmed, L. Li, Z. Zhao, C. Bao, M. Tur, S. Ashrafi, and A. Willner, "Experimental demonstration of a 200-Gbit/s free-space optical link by multiplexing Laguerre-Gaussian beams with different radial indices," Opt. Lett. **41**(15), 3447 (2016).
16. K. Dholakia, N. B. Simpson, M. J. Padgett, and L. Allen, "Second Harmonic Generation and the Orbital Angular Momentum of Light," Phys. Rev. A **54**(5), R3742–R3745 (1996).
17. X. Fang, D. Wei, Y. M. Wang, H. J. Wang, Y. Zhang, X. P. Hu, S. N. Zhu, and M. Xiao, "Conical third-harmonic generation in a hexagonally poled LiTaO3 crystal," Appl. Phys. Lett. **110**(11), 111105 (2017).
18. X. Fang, G. Yang, D. Wei, D. Wei, R. Ni, W. Ji, Y. Zhang, X. Hu, W. Hu, Y. Q. Lu, S. N. Zhu, and M. Xiao, "Coupled orbital angular momentum conversions in a quasi-periodically poled LiTaO3 crystal," Opt. Lett. **41**(6), 1169–1172 (2016).
19. X. Fang, D. Z. Wei, D. Liu, W. H. Zhong, R. Ni, Z. Chen, X. Hu, Y. Zhang, S. N. Zhu, and M. Xiao, "Multiple copies of orbital angular momentum states through second-harmonic generation in a two-dimensional periodically poled LiTaO3 crystal," Appl. Phys. Lett. **107**(16), 161102 (2015).
20. D. S. Ding, Z. Y. Zhou, B. S. Shi, X. B. Zhou, and G. C. Guo, "Linear up-conversion of orbital angular momentum," Opt. Lett. **37**(15), 3270 (2012).
21. J. Arlt, K. Dholakia, L. Allen, and M. J. Padgett, "Parametric down-conversion for light beams possessing orbital angular momentum," Phys. Rev. A **59**(5), 3950–3952 (1999).
22. M. Martinelli, J. A. O. Huguenin, P. Nussenzveig, and A. Z. Khoury, "Orbital angular momentum exchange in an optical parametric oscillator," Phys. Rev. A **70**(1), 013812 (2004).
23. D. Wei, J. L. Guo, X. Y. Fang, D. Z. Wei, R. Ni, P. Chen, X. P. Hu, Y. Zhang, W. Hu, Y. Q. Lu, S. N. Zhu, and M. Xiao, "Multiple generations of high-order orbital angular momentum modes through cascaded third-harmonic generation in a 2D nonlinear photonic crystal," Opt. Express **25**(10), 11556 (2017).
24. Y. Wang, D. Z. Wei, Y. Z. Zhu, X. Y. Huang, X. Y. Fang, W. H. Zhong, Q. J. Wang, Y. Zhang, and M. Xiao, "Conversion of the optical orbital angular momentum in a plasmon-assisted second-harmonic generation," Appl. Phys. Lett. **109**(8), 081105 (2016).
25. X. Fang, Z. Y. Kuang, P. Chen, H. C. Yang, Q. Li, W. Hu, Y. Lu, Y. Zhang, and M. Xiao, "Examining second-harmonic generation of high-order LG modes through a single cylindrical lens," Opt. Lett. **42**(21), 4387 (2017).
26. R. N. Lanning, Z. Xiao, M. Zhang, I. Novikova, E. E. Mikhailov, and J. P. Dowling, "Gaussian-beam-propagation theory for nonlinear optics involving an analytical treatment of orbital-angular-momentum transfer," Phys. Rev. A **96**(1), 013830 (2017).
27. R. W. Boyd, Nonlinear Optics, 3rd ed.(Academic Press, 2012).

OSA CONTINUUM

28. C. Schwob, P. F. Cohadon, C. Fabre, M. A. M. Marte, H. Ritsch, A. Gatti, and L. Lugiato, "Transverse effects and mode couplings in OPOs," Appl. Phys. B: Lasers Opt. **66**(6), 685–699 (1998).
29. L. J. Pereira, W. T. Buono, D. S. Tasca, K. Dechoum, and A. Z. Khoury, "Orbital-angular-momentum mixing in type-II second-harmonic generation," Phys. Rev. A **96**(5), 053856 (2017).
30. J. Lowney, T. Roger, D. Faccio, and E. M. Wright, "Dichroism for Orbital Angular Momentum using Stimulated Parametric Down Conversion," Phys. Rev. A **90**(5), 053828 (2014).

219.228.146.119 {ts '2019-01-29 23:20:45'}